INTERNATIONAL JOURNAL OF ADAPTIVE CONTROL AND SIGNAL PROCESSING
Int. J. Adapt. Control Signal Process. 2013; **27**:166–181
Published online 28 March 2012 in Wiley Online Library (wileyonlinelibrary.com). DOI: 10.1002/acs.2287

A signal processing adaptive algorithm for nonstationary power signal parameter estimation

Shazia Hasan [1], P. K. Dash [1,*,†] and S. Nanda [2]

[1] *Siksha O Anusandhan University, Bhubaneswar, India*
[2] *KIIT University, Bhubaneswar, India*

SUMMARY

This paper presents the design and analysis of an adaptive algorithm for tracking the amplitude, phase and frequency of the fundamental, harmonics and interharmonics present in time-varying power sinusoid in white noise. If frequency, amplitude and phase of the multiple sinusoids become nonstationary, they are estimated as an unconstrained optimization problem using robust and low complexity multi-objective Gauss–Newton algorithm. The presented algorithm deals with frequency drift and can accurately estimate frequency variation, amplitude and phase variation, as well as harmonic amplitude and phase variations. Further, the learning parameters in the proposed algorithm are tuned iteratively to provide faster convergence and better accuracy. The excellent tracking capability of proposed multi-objective Gauss–Newton algorithm is shown through simulation and experimental results in a nonstationary environment. Copyright © 2012 John Wiley & Sons, Ltd.

Received 25 July 2011; Revised 30 January 2012; Accepted 23 February 2012

KEY WORDS: sinusoids; amplitude and phase estimation; linear prediction; Newton method; Gauss–Newton method

1. INTRODUCTION

The problem of estimating the frequencies and other parameters of sinusoids in white noise is a classic one in radar, sonar, nuclear magnetic resonance (NMR), power networks, digital communication, analysis of earth waves, and so on, and has been extensively studied. Nonstationary sinusoids occur in electrical power networks owing to the proliferation of power electronic equipments, computers and microcontrollers, and result in the generation of harmonics, and interharmonics. These harmonic and interharmonic signals circulate in the electrical network and disturb the correct operation of electronic equipments and accelerate their degradation. To correctly assess the harmonic and interharmonic components in a distorted power signal, fast Fourier transform (FFT) [1], short time Fourier transform (STFT) are most often used. These transforms perform satisfactorily for stationary signals where properties of the signals do not change with time. For nonstationary signals, the STFT does not track the signal dynamics properly. Also, some of the FFT based windowed interpolation techniques have been presented [2–4] for harmonic and interharmonic estimation, and the accuracy of each of these algorithms is influenced by the choice of windowing function. Also, in estimating the fundamental and harmonic components of the voltage or current signal, the electrical system frequency f is assumed to remain constant at 50 or 60 Hz. However, in a power network, the fundamental system frequency seldom remains constant because of sudden load changes, and therefore, even a small frequency drift can influence the estimation accuracy of the various signal

*Correspondence to: P. K. Dash, Electrical Engineering Dept., Siksha O Anusandhan University, Khandagiri Square, Bhubaneswar, Odisha, India.
†E-mail: pkdash.india@gmail.com

components.Thus, the initial frequency of the signal needs to be estimated for accurate estimation of harmonic, interharmonic amplitude and phase angles. The estimated frequency of the noisy signal shall not be equal to the actual one when, the signal-to-noise ratio (SNR) of the signal is low and the frequency change from the original 50 or 60 Hz is substantial.

For accurate estimation of frequency and harmonics or interharmonics in the presence of noise, most of the algorithms are based on conventional signal processing techniques, such as recursive least squares [5,6], notch filters [7], Kalman filters [8,9], Neural networks [10,11], linear prediction [12], Newton methods [13–16], and other variants [17–19], and others. Although these techniques show very good results in fundamental and harmonic estimation, they suffer from large computational overhead and take more than two cycles (based on fundamental frequency of the signal) in converging to the desired estimation.

The Gauss–Newton methods depicted earlier [14, 15] do not estimate all the parameters of harmonically related sinusoids, the first, only frequency and the second, one amplitude and phase of a signal without harmonics or interharmonics. Thus, in this paper, a multi-objective Gauss–Newton (MGN) algorithm is presented to simultaneously estimate the fundamental frequency, harmonics, interharmonics and amplitude and phase of the power sinusoids. This algorithm estimates frequency using the linear predictor error properties, and the amplitude and phase are computed using the recursive Gauss–Newton procedure. Further, to improve the performance of proposed algorithm for nonstationary signals, an adaptive variable-forgetting factor is used. Section 2 of this paper presents the signal model and the multi-objective Gauss–Newton algorithm. In Section 3, the performance analysis of the proposed algorithm is presented. Simulation results are included to evaluate the performance of the proposed algorithm in Section 4. Finally, the conclusion is drawn in Section 5. Although power sinusoids have been used for signal parameter estimation, the proposed approach is a general one and can be used for any type of nonstationary signal comprising single or not harmonically related multiple frequency components.

2. PROBLEM FORMULATION

The problem of multiple sinusoidal parameter estimation is formulated for discrete-time noisy measurements as follows:

$$y(k) = s(k) + n(k), k = 0, 1, 2, \ldots\ldots, N-1 \tag{1}$$

$$\text{and} \quad s(k) = \sum_{r=1}^{R} A_r(k) \sin(w_r(k) + \phi_r(k)) \tag{2}$$

where, A_r, w_r and ϕ_r are unknown values that denote the amplitude, frequency and phase of the rth real-valued sinusoid, respectively, whereas $n(k)$ is an additive white Gaussian noise with unknown variance σ^2. The proposed algorithm for the estimation of frequency, amplitude, and phase of the sinusoids is presented as follows except for R (number of sinusoids), which can be obtained directly using discrete Fourier transform.

2.1. Multi-objective Gauss–Newton algorithm

In this section, a multi-objective algorithm has been outlined to estimate the time-varying frequency, amplitude and phase of the power signal buried in noise. Here, the different frequencies present in the power signal are identified using a recursive Newton-type algorithm, and then they are used to estimate the amplitude and phase of the signal using Gauss–Newton approach.

The R sinusoids in $s(k)$ can uniquely be expressed as a linear combination of its previous $2R$ samples as follows:

$$s(k) = -\sum_{i=1}^{2R} a_i s(k-i) \tag{3}$$

DOI: 10.1002/acs

where a_i are referred to as linear prediction coefficients. The relationship between w_r and a_i is given [12] as

$$\sum_{i=0}^{2R} a_i z^i = 0 \tag{4}$$

where $a_0 = 1$ and $a_i = a_{2R-i},\ i = 0, 1, 2, \ldots R$, and $z = \exp(\pm j w_r)$. The linear predictor coefficients a_i are first estimated, and then the frequency is estimated using Equation (4). With the use of linear predictor properties, the estimation error function is formulated as follows:

$$e_w(k) = \sum_{i=0}^{R-1} \tilde{a}_i (y(k-i) + y(k-2R+i)) + \tilde{a}_R y(k-R) \tag{5}$$

with $\tilde{a}_i$ denoting the optimized value of a_i, and here $\tilde{a}_0$ may not be fixed to unity. The parameter of interest can accurately be estimated by minimizing an exponentially weighted recursive cost function given as follows:

$$\varepsilon_1(k) = \sum_{i=0}^{k} \lambda_1^{k-i} e_w^2(i) \tag{6}$$

where $0 < \lambda_1 \leqslant 1$ is the forgetting factor. Taking the example of a signal comprising of just two sinusoids with different amplitude, phase and frequencies, where $R = 2$, the signal can be written as follows:

$$s(k) = A_1(k) \sin(w_1(k) + \phi_1(k)) + A_2(k) \sin(w_2(k) + \phi_2(k)) \tag{7}$$

For the estimation of frequencies of this signal using Equation (3), the linear predictor coefficients required are $a_0 = a_4,\ a_1 = a_3$ and a_2, and the estimation error for this signal from Equation (5) can be rewritten as

$$e_w(k) = \tilde{a}_0 (y(k) + y(k-4)) + \tilde{a}_1 (y(k-1) + y(k-3)) + \tilde{a}_2 y(k-2) \tag{8}$$

Hence, the parameter vector to be estimated is given by $\tilde{\theta}(k) = [\tilde{a}_0\ \tilde{a}_1\ \tilde{a}_2]^T$. As e_w is not linear in $\tilde{a}_0$, $\tilde{a}_1$ and $\tilde{a}_2$, owing to time-varying nature of the signal, hence, conventional recursive least squares algorithm cannot be applied to minimize (6). This paper uses recursive Gauss–Newton algorithm to minimize (6), and the equation for updating sinusoidal parameter using recursive Gauss–Newton algorithm is obtained as follows:

$$\tilde{\theta}(k) = \tilde{\theta}(k-1) - H^{-1}(k) \psi(k) e_w(k) \tag{9}$$

$$\text{and} \quad H(k) = \sum_{i=0}^{k} \lambda_1^{k-i} \psi(i) \psi^T(i) \tag{10}$$

where gradient vector ψ is given as

$$\psi(k) = \frac{\partial e_w(k)}{\partial \tilde{\theta}} = \begin{bmatrix} y(k) + y(k-4) \\ y(k-1) + y(k-3) \\ y(k-2) \end{bmatrix}, \tag{11}$$

and the Hessian matrix $H(k)$ can be written as follows:

$$H(k) = \sum_{i=0}^{k} \lambda_1^{k-i} \begin{bmatrix} (y(k)+y(k-4))^2 & (y(k)+y(k-4))(y(k-1)+y(k-3)) & (y(k)+y(k-4))(y(k-2)) \\ y(k)+y(k-4))(y(k-1)+y(k-3)) & (y(k-1)+y(k-3))^2 & (y(k-1)+y(k-3))(y(k-2)) \\ (y(k)+y(k-4))(y(k-2)) & (y(k-1)+y(k-3))(y(k-2)) & (y(k-2))^2 \end{bmatrix} \tag{12}$$

DOI: 10.1002/acs

To compute $H^{-1}(k)$, one can directly use the matrix inverse lemma. But, it is computationally expensive. The proposed algorithm reduces the computational complexity of the recursive Gauss–Newton method by modifying the conventional method. Assuming w not near to 0 or π, $H(k)$ can be approximated as follows:

$$H(k) = \sum_{i=0}^{k} \lambda_1^{k-i} \begin{bmatrix} (y(k)+y(k-4))^2 & 0 & 0 \\ 0 & (y(k-1)+y(k-3))^2 & 0 \\ 0 & 0 & (y(k-2))^2 \end{bmatrix} \tag{13}$$

Where

$$y(k)+y(k-4) = 2\,A_1(k-2)\cos(2w_1)\sin(w_1(k-2) + \phi_1(k-2)) + 2A_2(k-2)\cos(2w_2)\sin(w_2(k-2)+\phi_2(k-2)) \tag{14}$$

$$y(k-1)+y(k-3) = 2A_1(k-2)\cos(w_1)\sin(w_1(k-2) + \phi_1(k-2)) + 2A_2(k-2)\cos(w_2)\sin(w_2(k-2)+\phi_2(k-2)) \tag{15}$$

$$y(k-2) = A_1(k-2)\sin(w_1(k-2)+\phi_1(k-2)) + A_2(k-2)\sin(w_2(k-2)+\phi_2(k-2)) \tag{16}$$

Using these samples into Equation (13) and solving them, we get the Hessian matrix in the following form:

$$H(k) = \frac{1-\lambda_1^{k+1}}{2(1-\lambda_1)} \begin{bmatrix} 8A_1^2\cos^2(2w_1)\sin^2(w_1(k-2)+\phi_1(k-2)) + 8A_2^2\cos^2(2w_2)\sin^2(w_2(k-2)+\phi_2(k-2)) & 0 & 0 \\ 0 & 8A_1^2\cos^2(w_1)\sin^2(w_1(k-2)+\phi_1(k-2)) + 8A_2^2\cos^2(w_2)\sin^2(w_2(k-2)+\phi_2(k-2)) & 0 \\ 0 & 0 & 2A_1^2\sin^2(w_1(k-2)+\phi_1(k-2)) + A_2^2\sin^2(w_2(k-2)+\phi_2(k-2)) \end{bmatrix} \tag{17}$$

The terms (1,1), (2,2) and (3,3) of Equation (17) are denoted as X, Y, Z, respectively. The inverse of the Hessian matrix H^{-1} can easily be calculated as

$$H^{-1}(k) = \begin{bmatrix} 1/c(k)X & 0 & 0 \\ 0 & 1/c(k)Y & 0 \\ 0 & 0 & 1/c(k)Z \end{bmatrix} \tag{18}$$

where

$$c(k) = \frac{1-\lambda_1^{k+1}}{2(1-\lambda_1)} \tag{19}$$

Also, it can be observed that $c(k)$can be computed recursively as

$$c(k) = \lambda_1 c(k-1) + 1/2 \tag{20}$$

Further, by putting (18) and (19) into (9), the following equations are obtained:

$$\tilde{a}_0(k) = \tilde{a}_0(k-1) - e_w(k)(A_1(k-2)\cos(2w_1)\sin(w_1(k-2)+\phi_1(k-2)) + A_2(k-2)\cos(2w_2)\sin(w_2(k-2)+\phi_2(k-2)))/4c(k)X \tag{21}$$

$$\tilde{a}_1(k) = \tilde{a}_1(k-1) - e_w(k)(A_1(k-2)\cos(w_1)\sin(w_1(k-2)+\phi_1(k-2)) + A_2(k-2)\cos(w_2)\sin(w_2(k-2)+\phi_2(k-2)))/4c(k)Y \tag{22}$$

$$\tilde{a}_2(k) = \tilde{a}_2(k-1) - e_w(k)(A_1(k-2)\sin(w_1(k-2) + \phi_1(k-2)) + A_2(k-2)\sin(w_2(k-2)+\phi_2(k-2)))/2c(k)Z \tag{23}$$

Then, using Equation (4), the frequencies of two sinusoids can be computed as $\cos^{-1}\left(\frac{\tilde{a}_1 \pm \sqrt{\tilde{a}_1^2+2(\tilde{a}_2+2)}}{4}\right)$ [17].

After estimating frequency, the amplitude and phase of the signal are calculated using recursive Gauss–Newton method based on another objective function in the same iteration. For calculating

DOI: 10.1002/acs

amplitude and phase of the sinusoid, let the parameter vector be $\theta_r(k) = [A_r(k)\ \ \phi_r(k)]^T$ and its estimate be $\hat{\theta}_r(k) = [\hat{A}_r(k)\ \ \hat{\phi}_r(k)]^T$. Using $\hat{\theta}_r(k-1)$, the estimate of $y(k)$ at time k is computed as follows:

$$\hat{y}(k) = \sum_{r=1}^{R} \hat{A}_r(k-1)\ \sin(w_r k + \hat{\phi}_r(k-1)) \tag{24}$$

The a priori estimation error at time k is given as

$$e_\theta(k) = y(k) - \sum_{r=1}^{R} \hat{A}_r(k-1)\ \sin(w_r k + \hat{\phi}_r(k-1)) \tag{25}$$

and a similar exponentially weighted cost function is taken for updating the parameters as follows:

$$\varepsilon_2(k) = \sum_{i=0}^{k} \lambda_2^{k-i} e_\theta^2(i), 0 < \lambda_2 \leqslant 1 \tag{26}$$

In (26), λ_2 is also another forgetting factor. In this case, also the recursive Gauss–Newton method is used to minimize (26) in a similar manner as mentioned earlier.

The gradient vector and the Hessian matrix are given by Equations (27), and (28) respectively.

$$\psi_r(k) = \frac{\partial e_\theta(k)}{\partial \hat{\theta}} = \begin{bmatrix} -\sin(w_r k + \hat{\phi}_r(k-1)) \\ -\hat{A}_r(k-1)\cos(w_r k + \hat{\phi}_r(k-1)) \end{bmatrix} \tag{27}$$

$$H_r(k) = \sum_{i=0}^{k} \lambda_2^{k-i} \begin{bmatrix} \sin^2(w_r + \hat{\phi}_r(k-1)) & \hat{A}_r(k-1)\sin(2(w_r + \hat{\phi}_r(k-1)))/2 \\ \hat{A}_r(k-1)\sin(2(w_r + \hat{\phi}_r(k-1)))/2 & \hat{A}_r^2(k-1)\cos^2(w_r + \hat{\phi}_r(k-1)) \end{bmatrix} \tag{28}$$

Applying similar approximation outlined earlier, the Hessian matrix in (28) can be written as follows:

$$H_r(k) = \sum_{i=0}^{k} \lambda_2^{k-i} \begin{bmatrix} 1/2 & 0 \\ 0 & \hat{A}_r^2(k-1)/2 \end{bmatrix} = \frac{1-\lambda_2^{k+1}}{2(1-\lambda_2)} \begin{bmatrix} 1 & 0 \\ 0 & \hat{A}_r^2(k-1) \end{bmatrix} \tag{29}$$

And the inverse $H_r^{-1}(k)$ is computed as

$$H_r^{-1}(k) = \begin{bmatrix} 1/c(k) & 0 \\ 0 & 1/\hat{A}_r^2(k-1)c(k) \end{bmatrix} \tag{30}$$

where $c(k)$ is calculated as in Equation (20) with forgetting factor λ_2. Further, by putting (30) and (20) into (9), the amplitude and phase are calculated as follows:

$$\hat{A}_r(k) = \hat{A}_r(k-1) + \sin(\hat{w}_r(k-1)k + \hat{\phi}_r(k-1))e_\theta(k)/c(k) \tag{31}$$

$$\hat{\phi}_r(k) = \hat{\phi}_r(k-1) + \cos(\hat{w}_r(k-1)k + \hat{\phi}_r(k-1))e_\theta(k)/(\hat{A}_r(k-1)c(k)) \tag{32}$$

Thus, using Equations (21)–(23) and (31) and (32), frequency, amplitude, and phase of the fundamental, harmonic, and interharmonic components are estimated. The computation involves a few multiplication and divisions for each frequency in the signal, and the complexity is of the same order as adalines. The decoupled nature of the algorithm for the estimation of various amplitude and phase components is quite apparent from these equations.

From the previously mentioned equations, it is observed that the forgetting factors λ_1 and λ_2 influence the estimation process. When the signal is contaminated with high random noise, forgetting factor close to 0.5 results in faster convergence, but increased sensitivity to noise. However, using forgetting factor close to 1 (e.g., $\lambda = 0.99$) results in slow convergence, but better noise

DOI: 10.1002/acs

rejection property [18]. The forgetting factor is tuned according to the dynamics of the input signal [19, 20], and is given by the following:

$$\lambda_k = \lambda_0 + (1-\lambda_0)e^{(-z_k/z_0)} \tag{33}$$

and another variation is

$$\lambda_k = \lambda_0 + (\lambda_1-\lambda_0)e^{(-z_k/z_0)} \tag{34}$$

where

$$z_k = \sum_{i=0}^{k} e_\theta(i) \tag{35}$$

In the previously mentioned equations, λ_k and z_k are forgetting factor and sum of the residual error absolute values, respectively, and λ_0, λ_1, with $\lambda_0 \leqslant \lambda_1$ and z_0 are the tuning parameters. This paper proposes an adaptive tuning method using the covariance of the error signal as follows:

$$\begin{aligned}\lambda_{1(k)} &= \lambda_{1(k-1)} + (1-\lambda_{1(k-1)})\exp(-e_w(k)e_w(k-1))\\ \lambda_{2(k)} &= \lambda_{2(k-1)} + (1-\lambda_{2(k-1)})\exp(-e_\theta(k)e_\theta(k-1))\end{aligned} \tag{36}$$

where $e_w(k), e_\theta(k), e_w(k-1)$ and $e_\theta(k-1)$ are the a priori estimation errors at time k and $k-1$, respectively. Since this tuning method uses the present and past errors combining them as a covariance function, it is expected to provide better accuracy in tracking during sudden step changes of parameters, and changes of the network topology, and others. Thus, if the covariance is large, the forgetting factor according to Equation (36) is close to the initial small value, providing fast convergence. However, when the convergence is achieved, the covariance is small, thus making the forgetting factor close to 1, providing better sensitivity to noise. The major steps for computing the proposed algorithm is summarized in Figure 1 where th1 and th2 are taken to be a small positive quantity.

3. PERFORMANCE ANALYSIS OF THE PROPOSED ALGORITHM

In this section, the mean-square estimation error of the parameters under stationary condition is analyzed. Considering the signal parameters represented as $\theta = [a_0, a_1, a_2, A_r, \phi_r]^T$, the covariance matrix in MGN method denoted as $\mathrm{cov}(\hat{\theta}(k))$, is calculated for two different objective functions as follows:

$$\begin{aligned}\mathrm{cov}(\hat{\theta}(k)) &= E\left\{\left[\frac{\partial\varepsilon_1^2(k)}{\partial\hat{\theta}^2}\right]^{-1}\left[\frac{\partial\varepsilon_1(k)}{\partial\hat{\theta}}\right]\left[\frac{\partial\varepsilon_1(k)}{\partial\hat{\theta}}\right]^T\left[\frac{\partial\varepsilon_1^2(k)}{\partial\hat{\theta}^2}\right]^{-1}\right\}_{\hat{\theta}(k)=\theta}\\ &= \sigma^2\left[\sum_{i=0}^{k}\lambda_1^{k-i}\psi(i)\psi^T(i)\right]^{-1}\times\sum_{i=0}^{k}\lambda_1^{2(k-i)}\psi(i)\psi^T(i)\quad\times\left[\sum_{i=0}^{k}\lambda_1^{k-i}\psi(i)\psi^T(i)\right]^{-1}\end{aligned} \tag{37}$$

where E denotes the expectation operation. When k is sufficiently large, we obtain the following:

$$\mathrm{cov}(\hat{\theta}(k)) \approx \sigma^2\begin{bmatrix}\frac{1}{c(k)X} & 0 & 0\\ 0 & \frac{1}{c(k)Y} & 0\\ 0 & 0 & \frac{1}{c(k)Z}\end{bmatrix} \tag{38}$$

hence, the variance of the linear predictor coefficients are given as follows:

$$\mathrm{var}(\tilde{a}_0(k)) = \frac{\sigma^2(1-\lambda_1)}{4(1-\lambda_1^{k+1})(A_1^2\cos^2(2w_1)\sin^2(w_1(k-2)+\phi_1(k-2)) + A_2^2\cos^2(2w_2)\sin^2(w_2(k-2)+\phi_2(k-2)))} \tag{39}$$

$$\mathrm{var}(\tilde{a}_1(k)) = \frac{\sigma^2(1-\lambda_1)}{4(1-\lambda_1^{k+1})(A_1^2\cos^2(w_1)\sin^2(w_1(k-2)+\phi_1(k-2)) + A_2^2\cos^2(w_2)\sin^2(w_2(k-2)+\phi_2(k-2)))} \tag{40}$$

DOI: 10.1002/acs

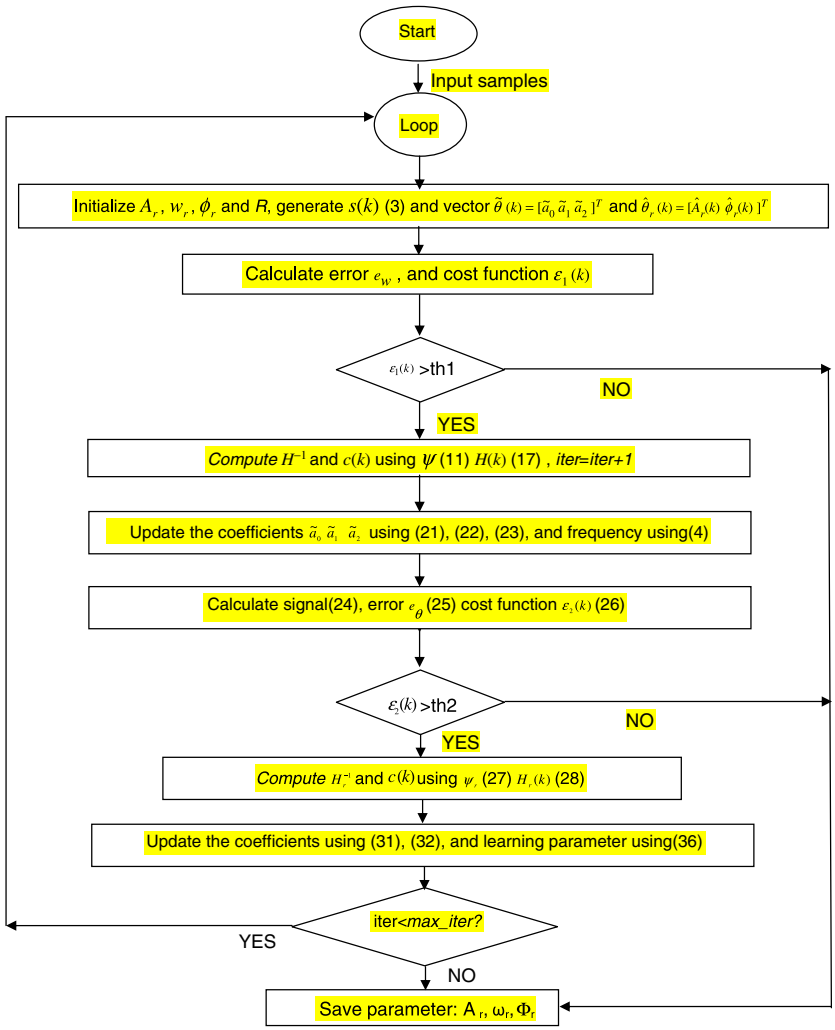

Figure 1. Summary of the major steps for computing the proposed algorithm.

and

$$\mathrm{var}(\tilde{a}_2(k)) = \frac{\sigma^2(1-\lambda_1)}{2(1-\lambda_1^{k+1})(A_1^2\sin^2(w_1(k-2)+\phi_1(k-2)) + A_2^2\sin^2(w_2(k-2)+\phi_2(k-2)))} \tag{41}$$

Similarly, analyzing $\mathrm{cov}(\hat{\theta}(k))$ for the second cost function, the variance of the amplitude and phase are found to be

$$\mathrm{var}(\hat{A}_r(k)) = \frac{2\sigma^2(1-\lambda_2)}{(1-\lambda_2^{k+1})} \tag{42}$$

and

$$\mathrm{var}(\hat{\phi}_r(k)) = \frac{2\sigma^2(1-\lambda_2)}{A^2(1-\lambda_2^{k+1})} \tag{43}$$

If all the forgetting factors are made equal to unity, then the variances will attain their Cramer–Rao lower bound for sufficiently large values of k and with $\eta(k)$ considered as a Gaussian distributed noise. Hence, it is proved that the MGN algorithm attains optimal performance for stationary amplitude, phase and frequency in an asymptotic sense.

DOI: 10.1002/acs

4. SIMULATION RESULTS

Computer simulations have been carried out to evaluate the performance of the proposed algorithm.

A. Case 1.

The first experiment is done for the estimation of power signal with abrupt frequency change. The signal frequency changes from 50 to 45 Hz. The signal is tested for comparing the accuracy of the proposed tuning method. The power signal is represented as

$$y(k) = A(k)\ \sin(w(k)k + \phi(k)) + n_k \tag{44}$$

In this case, the sampling frequency is taken to be 1 kHz, as the interest lies in computing the fundamental frequency changes. Figure 2(a) shows clearly the accurate tracking capability of the proposed adaptive tuning method (given in Equation (36)) in comparison with the other two methods (given in Equations (33) and (34)). Hence, for the rest of the analysis, the proposed tuning method is used. Now, for comparing the effect of different sampling rates, the test signal given in Equation (44) with constant frequency of 50 Hz and amplitude 1.0 pu. is considered. First, the signal parameters are estimated using 1 kHz sampling rate, and then the test signal is applied to a sampling rate of 6.4 kHz to the proposed MGN algorithm with the adaptive tuning method. Figure 2(b) clearly shows that both the estimation converges almost in the same time. For real time estimation of fundamental components the sampling rate should be kept small whereas for harmonic estimation, a higher sampling rate can be used.

Case 2

The second experiment is performed for the estimation of power signal, which includes step change in frequency, amplitude and phase for obtaining the percentage estimation error for different algorithms that include extended Kalman filter (EKF) [9], two-stage adaline [11], supervised Gauss–Newton algorithm [13], multi-objective Gauss–Newton with constant forgetting factor, and adaptively tuned MGN for different noise levels. The power signal considered for the test is the same as that given in Equation (44). The initial forgetting factor is $\lambda_1 = \lambda_2 = 0.55$. For the first 70 samples, $\mathrm{freq} = 60$ Hz, $A = 1$ pu, $\Phi = \pi/4$; for 70 to 150 sample parameter change to $\mathrm{freq} = 59.5$ Hz, $A = 1.2$pu, $\Phi = \pi/6$, after which they take their initial values of amplitude and phase with $\mathrm{freq} = 59.7$ Hz. To test the noise sensitivity of the proposed adaptive filter additive white Gaussian noise (AWGN) [20, 21] of SNR varying from 10 to 40 dB is considered. The SNR is defined as follows:

$$\mathrm{SNR\ (dB)} = 10\log(P_s/P_n) = 20\log(\mathrm{A}/\sqrt{2}\sigma) \tag{45}$$

where P_s is the power of the signal and P_n is the noise power, A is amplitude of the signal and σ standard deviation of noise signal. A 30-dB noise indicates a peak noise magnitude of 3.1% (variance$\sigma^2 = 0.0005$) of the signal, whereas a noise of 10 dB is equivalent to nearly 31% (variance$\sigma^2 = 0.05$) of the signal peak amplitude. The performance of the algorithm is tested with high-noise condition of 10 dB as shown in Figure 3.

From the simulation results, it is clear that the proposed MGN with adaptive forgetting factor shows better noise rejection capability in comparison with the MGN algorithm with constant forgetting factor set to $\lambda_1 = \lambda_2 = 0.55$. The comparison of the percentage estimation error of different algorithms for different noise levels for this test signal is presented in Table I. The program is run on a computer with CPU: Intel Pentium 2.00 GHz and Memory: 760 MB (Sta. Clara, CA, USA). Table II gives the one-step iterative calculation time of different algorithms for this test signal, and from this table, it is clear that the proposed MGN method with adaptively tuned forgetting factor provides significant accuracy in the estimation of amplitude, phase and frequency of a 60-Hz power signal.

DOI: 10.1002/acs

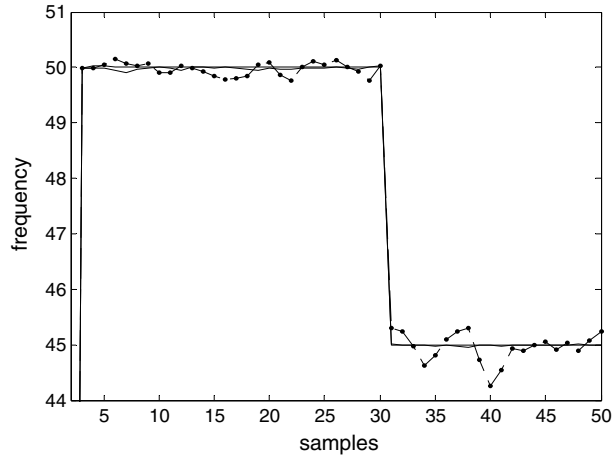

(a) Comparison of different tuning methods case:1: Method1 (dash-dot), method2 (dashed), proposed adaptive tuning (solid) (solid)

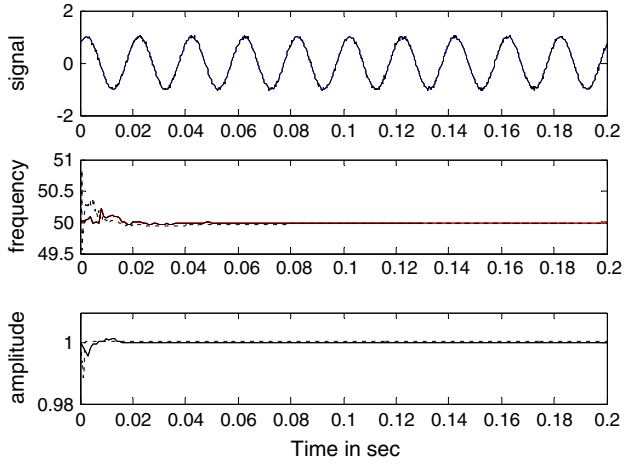

(b) Comparison of different sampling rate case:1: 1kHz(solid), 6.4kHz(dashed)

Figure 2. (a) Comparison of different tuning methods Case 1: method 1 (dash-dot), method 2 (dashed), proposed adaptive tuning (solid line); and (b) comparison of different sampling rate Case 1: 1 kHz (solid line), 6.4 kHz (dashed).

Case 3. Harmonic tracking of static signal

A harmonically related signal in noise is used for the estimation of the third, seventh, ninth and 13th harmonic components, which is typical in industrial load comprising power electronic converters and arc furnaces [10–12].

$$y(k) = 5\ \sin(\omega k T_s + 45^0) + 1.5\ \sin(3^*\omega k T_s + 36^0)\ + 0.85\ \ \sin(7^*\omega k T_s + 30^0) + 0.75\ \sin(9^*\omega k T_s + 25^0)\ + 0.5\ \ \sin(13^*\omega k T_s + 22^0) + n_k \tag{46}$$

This test signal has fundamental frequency equal to 60 Hz and a zero mean white Gaussian noise with $SNR = 30$ dB (variance $\sigma^2 = 0.0005$) is added to this test signal. A sampling frequency of 7.68 kHz is chosen with a view that the algorithm can estimate up to the 64th harmonic component present in the signal. Figure 4(a) and (b) shows the estimated frequency, amplitude and phase of the seventh and 13th harmonic components, respectively, and it is obvious from the figure that fast convergence to their true values (less than a cycle) and accuracy in estimation are achieved using

DOI: 10.1002/acs

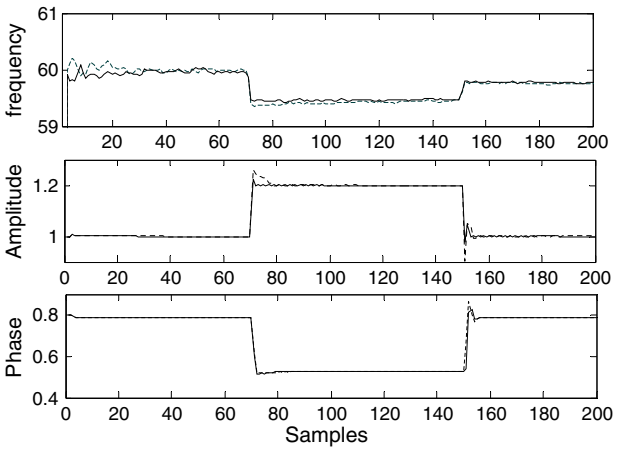

Figure 3. Estimation of all the parameters of case 2, multi-objective Gauss–Newton (dotted line), adaptive multi-objective Gauss–Newton (solid line).

Table I. Comparison of the percentage estimation error of different algorithms for different noise levels for the test signal.

Algorithm	Noise in (%)	Frequency error (%)	Amplitude error (%)	Phase
EKF	3.16	0.3026	1.080	0.547
	10.00	0.4040	3.900	4.070
	31.60	2.1160	6.090	6.520
Two-stage adaline	3.16	0.0030	0.991	0.032
	10.00	0.0970	1.730	0.179
	31.60	0.5360	2.010	0.972
Supervised	3.16	0.0046	0.781	0.050
Gauss–Newton algorithm	10.00	0.1024	1.020	0.120
	31.60	0.6210	1.400	0.990
MGN with constant	31.6	0.0042	0.700	0.025
forgetting factor	10.00	0.0768	1.120	0.089
	31.60	0.4060	1.360	0.820
MGN with adaptively	3.16	0.0024	0.500	0.021
tuned forgetting factor	10.00	0.0642	0.870	0.089
	31.60	0.2030	1.090	0.793

EKF, extended Kalman filter; MGN, multi-objective Gauss–Newton.

Table II. One-step iterative calculation time of different algorithms for the test signal.

Algorithm (ms)	Time (ms)
EKF	1.49
Two-stage adaline	0.81
Supervised Gauss–Newton algorithm	0.78
MGN with constant forgetting factor	0.7
MGN with adaptive tuning	0.75

EKF, extended Kalman filter; MGN, multi-objective Gauss–Newton.

the proposed adaptively tuned MGN algorithm. The algorithm is very fast as it does not invert a Jacobean similar to the normal Gauss–Newton method [14].

DOI: 10.1002/acs

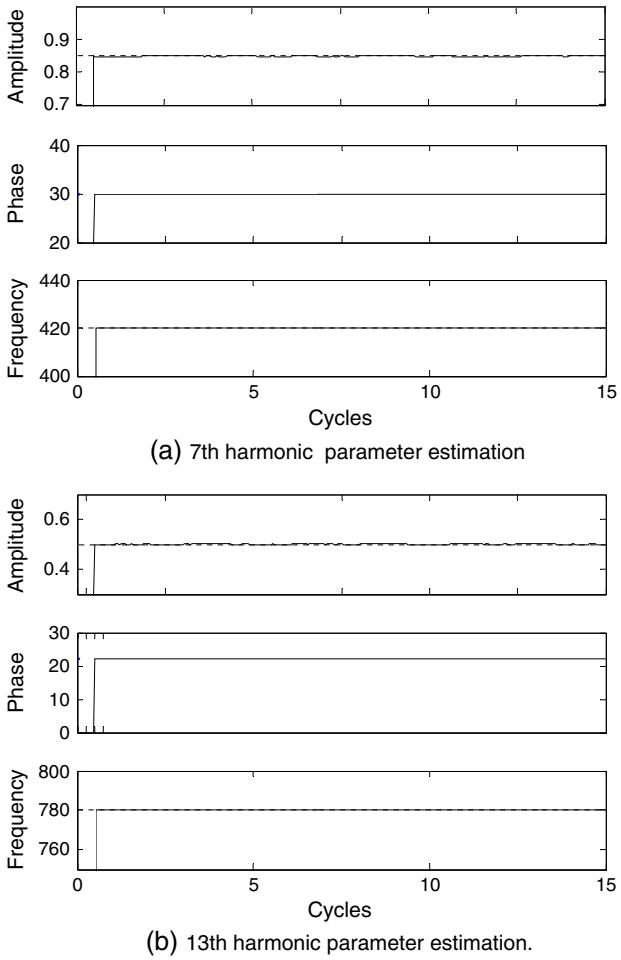

Figure 4. (a) Seventh and (b) 13th harmonic parameter estimations.

Case 4. Harmonic and interharmonic estimation

The test power signal is assumed to comprise a fundamental, several harmonics and two interharmonics and is expressed as follows:

$$y(k) = 5\ \sin(\omega k T_s + \pi/4) + 1.5\ \sin(3^*\omega k T_s + \pi/4)\ + 0.75\ \sin(7^*\omega k T_s + \pi/4) \\ +0.5\ \sin(285^* k T_s + \pi/7) + 0.85\ \sin(510^* k T_s + \pi/4) + n_k \tag{47}$$

The frequency of the fundamental component of the previously mentioned signal is 50 Hz, and two interharmonic frequencies are 285 and 510 Hz, respectively. The estimated parameters of the interharmonic components are shown in Figure 5(a) and (b), respectively. From the figures, it is clear that the proposed algorithm with the variable forgetting factor takes less than two cycles for the estimation of interharmonics. The accuracy in estimation of all the parameters is given in Table III.

B. Experimental results

To evaluate the performance of the proposed algorithm in a real-time environment, a laboratory setup has been used to capture real-time nonstationary signal data. The estimation algorithm originally developed using MATLAB (MathWorks, Natick, MA, USA), is now reformulated with the LAB VIEW (National Instruments, Austin, Texas) software. The static as well as the dynamic performance of the proposed algorithm is tested using this software.

DOI: 10.1002/acs

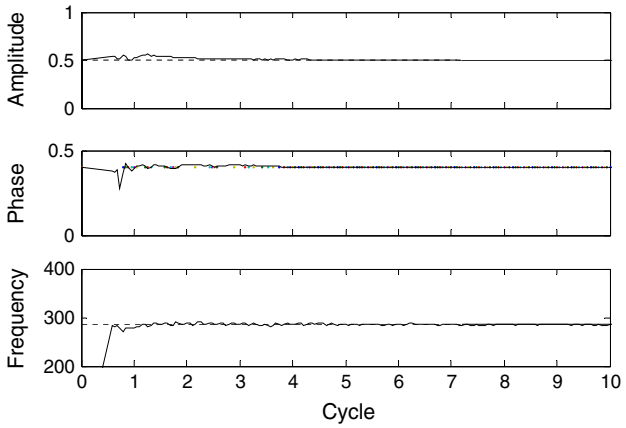

(a) 1st Inter harmonic parameter estimation.

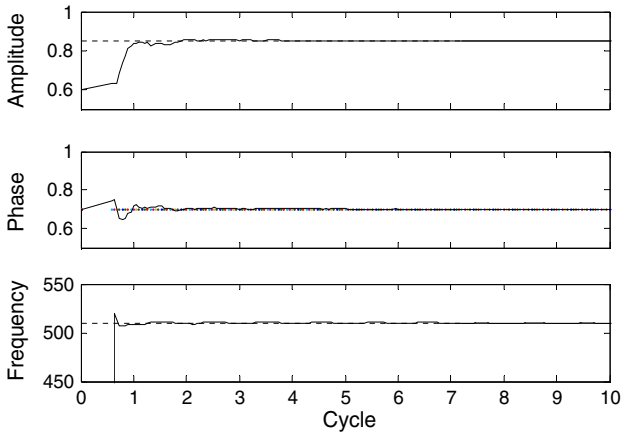

(b) 2nd Inter harmonic parameter estimation

Figure 5. (a) First and (b) second interharmonic parameter estimations.

Case 5

The fifth experiment is performed to test static performance of the proposed algorithm in real-time environment. The recorded signal contains up to the 30th odd harmonic components, with fundamental frequency of 30 Hz, and is modeled as follows:

$$y(k) = \sum_{n=1}^{29} A_n \sin(n\omega_0 k T_s + \phi_n) \tag{48}$$

The fundamental and the harmonic amplitude and phase of the signal is estimated using the proposed algorithm using LAB VIEW software. Figure 6(a) shows the recorded real-time signal. Figure 6(b) shows the estimated fundamental components of the signal, and Figure 6(c) shows the 25th harmonic component of the signal. From the figure, it is clear that the proposed algorithm can efficiently estimate the real-time signal in a laboratory setup.

Case 6

The sixth experiment is performed to test the dynamic performance of the proposed algorithm in real-time environment using a highly distorted damped sinusoid with harmonics and corrupted with 30 dB (variance $\sigma^2 = 0.0005$) noise.

DOI: 10.1002/acs

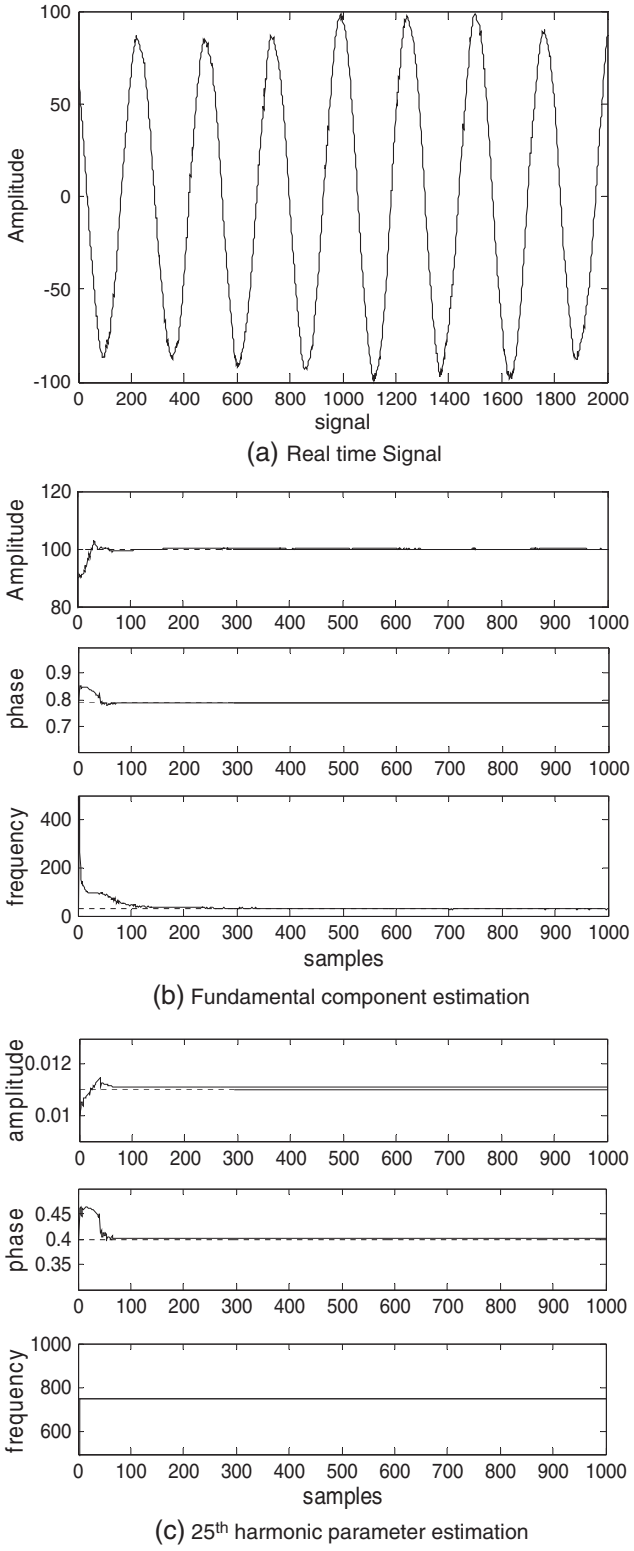

Figure 6. (a) Recorded real-time signal, (b) fundamental component estimation, and (c) 25th harmonic parameter estimation.

DOI: 10.1002/acs

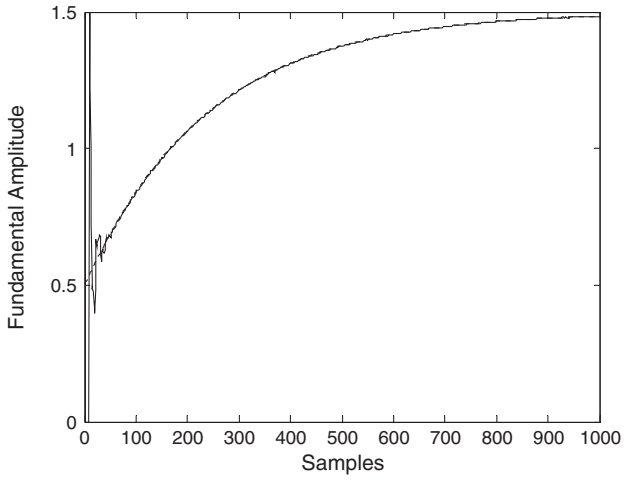

(a) Fundamental amplitude

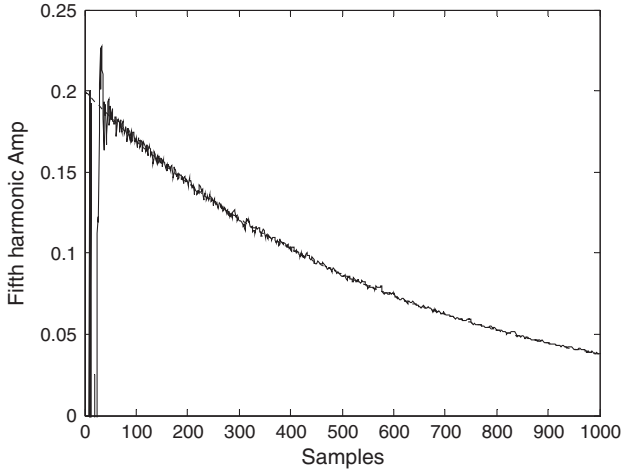

(b) Fifth harmonic amplitude

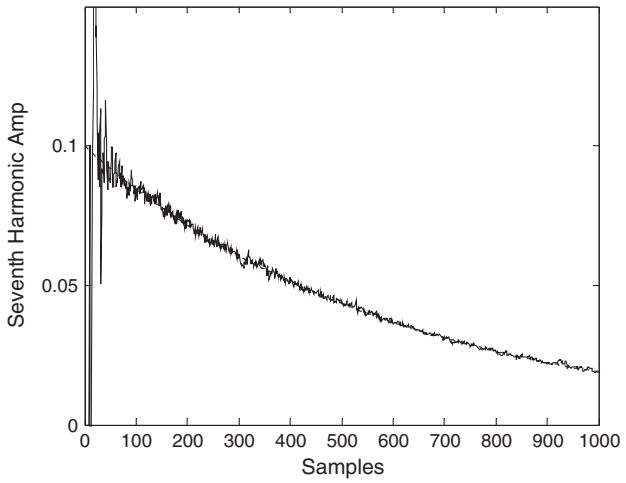

(c) Seventh harmonic amplitude

Figure 7. (a) Fundamental amplitude, (b) fifth, and (c) seventh harmonic amplitudes.

DOI: 10.1002/acs

Table III. Accuracy in estimation of all the parameters.

Order of harmonic and interharmonic	Estimated frequency	Frequency error (%)	Estimated amplitude	Amplitude error (%)	Estimated phase	Phase error (%)
Fundamental frequency	60.0061	0.0101	5.0001	0.0020	0.8002	0.025
Third harmonic	179.9694	0.0170	1.4993	0.046	0.5999	0.0166
Interharmonic	284.9571	0.0150	0.5001	0.020	0.4001	0.025
Seventh harmonic	419.9991	0.0230	0.7493	0.0930	0.5003	0.060
Interharmonic	509.9932	0.0019	0.8501	0.011	0.7004	0.0517

The damped sine wave with harmonic is modeled as follows:

$$y(k) = \left(A_1 - A_2 e^{-\alpha_1 k T_s} \right) \sin(\omega_0 k T_s + \phi_1(k)) + \sum_{n=3}^{9} A_n e^{-\alpha_n k T_s} \sin(n\omega_0 k T_s + \phi_n(k)) \tag{49}$$

and the parameters are set as initial forgetting factor, $\lambda_1 = \lambda_2 = 0.85$. The fundamental frequency is 50 Hz, and the amplitude and phase angle of the various components are chosen as $A1 = 1.5$ pu, $A2 = 1$ pu, $A3 = 0.5$ pu, $A5 = 0.2$ pu, $A7 = 0.1$ pu, $A9 = 0.05$ pu, $\alpha 1 = 5$, $\alpha 3 = \alpha 5 = \alpha 7 = \alpha 9 = 2$, $\phi_1 = 0.8$, $\phi_3 = 0.4$, $\phi_5 = 0.7$ $\phi_7 = 0.6$, $\phi_9 = 0.5$. Figure 7(a)–(c) shows fundamental fifth and seventh harmonic amplitude components of the estimated signal, respectively. From the figure, it is clear that the proposed algorithm outperforms even the estimation of such a complex signal in a laboratory setup.

5. CONCLUSION

This paper presents a robust adaptive multi-objective Gauss–Newton algorithm for the estimation of amplitude, phase and frequency of multiple time-varying power sinusoids buried in noise. For power sinusoids, where all the above parameters vary, a multi-objective algorithm produces the best convergence and least tracking error even in the presence of strong Gaussian white noise with low SNR. To highlight the robust tracking property of the proposed approach, several computational experiments have been presented that includes power frequencies of single and multiple sinusoids with step changes in amplitude, frequency and phase. Also the tracking of damped sinusoids with relatively much less computational burden has been presented with high accuracy. The time required for convergence of the signal parameters to their true values with different SNR is less than a cycle. The proposed algorithm has also been tested for real-time signals producing accurate tracking results within a time period of less than two cycles based on the fundamental frequency component.

REFERENCES

1. Girgis AA, Hann FM. A quantitative study of pitfalls in FFT. *IEEE Transactions on Aerospace and Electronics System* 1998; **44**(1):107–115.
2. Testa A, Gallo D, Langella R. On the processing of harmonics and interharmonics: using Hanning window in standard framework. *IEEE Transactions on Power Delivery* 2004; **19**(1):28–34.
3. Gallo D, Langella R, Testa A. Desynchronized processing technique for harmonic and interharmonics analysis. *IEEE Transactions on Power Delivery* 2004; **19**(3):993–1001.
4. Qian H, Zhao R, Chen T. Interharmonics analysis based on interpolating windowed FFT algorithm. *EEE Trans. Power Del* 2007; **22**(2):1064–1079.
5. Joorabian M, Mortazavi SS, Khayyami AA. Harmonic estimation in a power system using a novel hybrid least squares adaline algorithm. *Electric power System Research* 2009; **79**:107–116.
6. Mishra S. Hybrid least squares adaptive bacterial foraging strategy for harmonic estimation. *IEE Proceedings : Generation, Transmission, Distribution* 2005; **152**(3):379–389.
7. Niedzwickei M, Kaczmarek P. Tracking analysis of a generalized notch filters. *IEEE Transactions on Signal Processing* 2006; **54**(1):304–314.

DOI: 10.1002/acs

8. Routray A, Pradhan AK, Rao KP. A novel Kalman filter for frequency estimation of distorted signals in power system. *IEEE Transactions on Instrumentation and Measurement* 2002; **51**(3):469–479.
9. Costa FF, Cardoso AJM, Fernandes DA. Harmonic analysis based on Kalman filtering and prony's method. In *Proceedings, International Conference on Power Engineering, Energy Electrical Drives*: Setúbal, Portugal, April 12-14, 2007; 696–701.
10. Lin HC. Intelligent neural network-based fast power system harmonic detection. *IEEE Transactions on Industrial Electronics* 2007; **54**(1):43–52.
11. Chang GW, Chen C-I, Liang Q-W. A two-stage adaline for harmonics and interharmonics measurement. *IEEE Transactions on Industrial Electronics* 2009; **56**(6):2220–2228.
12. So HC, Chan KW, Chan YT, Ho KC. Linear prediction approach for efficient frequency estimation of multiple sinusoids: algorithms and analysis. *IEEE Transactions on Signal Processing* 2005; **53**(7):2290–2305.
13. Xue SY, Yang SX. Power system frequency estimation using supervised Gauss–Newton algorithm. *Measurement* 2009; **42**:28–37.
14. Yang J, Xi H, Guo W. Robust modified Newton algorithm for adaptive frequency estimation. *IEEE Signal processing letters* 2007; **14**(11):879–882.
15. Zheng J, Lui KWK, Ma WK, So HC. Two Simplified recursive Gauss–Newton algorithms for direct amplitude and phase tracking of a real sinusoid. *IEEE Signal Processing letters* 2007; **14**(12):972–975.
16. Terzija VV. Improved recursive Newton-type algorithm for frequency and spectra estimation in power systems. *IEEE Transactions on Instrumentation and Measurement* 2003; **52**(5):1654–1659.
17. Yazdani D, Bakhshai A, Joos G, Mojiri M. A real-time extraction of harmonic and reactive current in nonlinear load for grid-connected converters. *IEEE Transactions on Industrial Electronics* 2009; **56**(6):2185–2189.
18. Lin HC. Fast tracking of time-varying power system frequency and harmonics using iterative-loop approaching algorithm. *IEEE Transactions on Industrial Electronics* 2007; **54**(2):974–983.
19. de Souza HEP, Bradaschia F, Neves FAS, Cavalcanti MC, Azevedo GMS, de Aruda JP. A method for extracting the fundamental frequency, positive sequence voltage vector based on simple mathematical transformations. *IEEE Transactions on Industrial Electronics* 2009; **56**(5):1539–1547.
20. Mojiri M, Karimi-Ghartemani M, Bakhshai A. Processing of harmonics and interharmonics using an adaptive notch filter. *IEEE Transactions on Power Delivery* 2010; **25**(2):534–542.
21. Zhang H, Liu P, Malik OP. Detection and classification of power quality disturbances in noisy conditions. *IEE Proceedings : Generation, Transmission, Distribution* 2003; **50**(5):567–572.

DOI: 10.1002/acs